

Strain Mode of General Flow: Characterization and Implications for Flow Pattern Structures

Yasuya Nakayama^{1,*}, Tatsunori Masaki², and Toshihisa Kajiwara¹

¹*Department of Chemical Engineering, Kyushu University, Nishi-ku, Fukuoka 819-0395, Japan and*

²*Development and Production Department, UNITIKA Ltd.,*

31-3, Uji-Hinojiri, Uji-shi, Kyoto 611-0021, Japan

(Dated: March 21, 2017)

Understanding the mixing capability of mixing devices based on their geometric shape is an important issue both for predicting mixing processes and for designing new mixers. The flow patterns in mixers are directly connected with the modes of the local strain rate, which is generally a combination of elongational flow and planar shear flow. We develop a measure to characterize the modes of the strain rate for general flow occurring in mixers. The spatial distribution of the volumetric strain rate (or non-planar strain rate) in connection with the flow pattern plays an essential role in understanding distributive mixing. With our measure, flows with different types of screw elements in a twin-screw extruder are numerically analyzed. The difference in flow pattern structure between conveying screws and kneading disks is successfully characterized by the distribution of the volumetric strain rate. The results suggest that the distribution of the strain rate mode offers an essential and convenient way for characterization of the relation between flow pattern structure and the mixer geometry.

Keywords: Polymer processing, Food processing, Extrusion, Distributive mixing, Twin-screw extruder, Simulation

I. INTRODUCTION

Mixing is one of the most important process in industries, including polymer processing, rubber compounding, and food processing, because it directly affects the quality of multi-component materials [1–4]. Several types of mixing devices, such as twin-screw extruders, twin-rotor mixers, and single-screw extruders, have been developed for different material processabilities and different processing purposes. To select an appropriate mixing element for a variety of complex materials and product qualities, one fundamental issue is the fluid mechanical characterization of the mixing capability of various types of the mixing elements.

The mixing process, or, more specifically, the reduction of the inhomogeneity of material mixtures, is achieved through material flow driven by mixing devices. Therefore, in principle, the capability of the mixing elements can be evaluated through an analysis of the flow in the device. Along these lines, the visualization of the flow patterns has been performed numerically or experimentally to obtain a qualitative insight into the global mixing kinetics [5–11]. While the global flow pattern characterizes the evolution of the material distribution, the divergence of the material trajectories is locally associated with the deformation of the fluid elements. Since the substantial local deformation rate is described by the strain rate tensor, several approaches for the characterization of the local strain rate have been developed [12–15].

The degree of irrotationality of the deformation rate, which is often called the “mixing index” [16], has been

used to quantify dispersive mixing efficiency [13, 14]. This characterization was motivated by the experimental fact that elongational flows are more effective than simple shear for droplet/agglomerate breakup. In a rheometric flow setup, the elongational flows are irrotational, while the simple shear flow is a superposition of a planar shear flow and a rotational flow in a plane. Therefore, the irrotationality can define the flow type for the rheometric flow setup. However, in generic flows in mixing devices, the type of elongational flows described by the strain rate tensor cannot be assessed by the irrotationality by definition. Another quantity, called the mixing efficiency, is the relative magnitude of the elongational rate along a certain direction to the magnitude of the strain rate tensor [12, 13]. The mixing efficiency is useful when the interface between phases is well defined. If, in the mixing efficiency, the maximal elongational direction is taken, the modes of the strain rate, such as the uniaxial/biaxial elongational flows and the planar shear flow, are discriminated [15]. In this case, the eigenvalue problem for the strain rate tensor should be solved. The distribution of the strain-rate modes in combination of the magnitude of the strain-rate in general flows should be useful in understanding the dispersive mixing capability. The strain-rate modes in three-dimensional flows can be identified in principle by combining the different eigenvalues of the strain-rate tensor, and thus different forms for quantification of the strain-rate mode can be designed. However, such quantification has not been derived in a numerically tractable manner.

To the best of our knowledge, the role of elongational flow in distributive mixing has been only rarely discussed, whereas the effectiveness of irrotational elongational flows for dispersive mixing has been well recognized. Flow trajectories diverge by elongational flows

* nakayama@chem-eng.kyushu-u.ac.jp

however small the elongational rate is. The divergence directions are restricted to a plane for planar shear flow, but involve three directions for non-planar elongational flows. If distributive mixing is effectively promoted in the confined space of a mixing device during a finite period of time, a flow pattern being effective to distributive mixing should be developed. Such a flow pattern is expected to be associated with a certain distribution of the non-planar or volumetric elongational flows. The distribution of the volumetric flows is therefore considered to give essential information for a better understanding of the mixing capability of mixing elements.

Especially, the flow patterns in the regions of smaller strain rates largely determine net mixing capabilities of mixing devices. Although the area-stretching ability is very low in the small strain rate regions, such regions occupy a large fraction of the channel, and the materials are conveyed to larger strain rate regions by the flow in the small strain rate regions. The distribution of the volumetric flows is expected to be useful in understanding the relation between the structure of the flow patterns in the small strain regions and the mixer geometry.

In general, the flow field in a mixing device is an arbitrary combination of volumetric elongational flows and a planar shear flow. Thus, for a general three-dimensional flow, rather than only rheometric flows, the characterization of volumetric elongational flows from the strain rate tensor is required. Although the strain-rate mode should be an important quantity both in dispersion capability and analysis of flow-pattern structures in relation to distributive mixing, its characterization in three-dimensional flows has not established so far.

In this paper, we derive a measure which identifies the volumetric elongational flows from the strain rate tensor. We apply this measure to melt-mixing flow in twin-screw extrusion. Using the distribution of the volumetric elongational flows, we discuss the differences in the flow patterns and the mixing characteristics of the different screw elements.

II. THEORY

In any kind of flow in a mixing device, the local deformation rate is a combination of shear flow, elongational flow, and rotational flow. The deformation rate of a fluid element, $\nabla \mathbf{v}$, is decomposed into the strain rate tensor \mathbf{D} and the vorticity tensor $\mathbf{\Omega}$:

$$\nabla \mathbf{v} = \mathbf{D} + \mathbf{\Omega}, \quad (1)$$

where \mathbf{v} is the velocity field, $\mathbf{D} = (\nabla \mathbf{v} + \nabla \mathbf{v}^T) / 2$, and $\mathbf{\Omega} = (\nabla \mathbf{v} - \nabla \mathbf{v}^T) / 2$, the superscript T indicates the transpose. Concerning mixing processes, the change in the distance between two nearby points is represented by \mathbf{D} . Thus, the strain rate tensor is mainly responsible for the local mixing capability.

For incompressible flows, *i.e.*, $\text{tr} \mathbf{D} = 0$, the strain rate tensor can be diagonalized with an orthonormal matrix

\mathbf{P} ,

$$\mathbf{D} = \mathbf{P}^T \cdot \mathbf{\Lambda} \cdot \mathbf{P}, \quad (2)$$

$$\mathbf{\Lambda} = \begin{pmatrix} \dot{\epsilon} & 0 & 0 \\ 0 & (m-1)\dot{\epsilon} & 0 \\ 0 & 0 & -m\dot{\epsilon} \end{pmatrix}, \quad (3)$$

where $\dot{\epsilon} > 0$ and $-m\dot{\epsilon}$, respectively, represent the largest and the smallest eigenvalues of \mathbf{D} by assuming $1/2 \leq m \leq 2$. The value of m specifies the mode of the strain rate. For example, $m = 1/2$ for a uniaxial elongational flow, $m = 2$ for a biaxial elongational flow, and $m = 1$ for a planar shear flow.

A typical value of the strain rate is $\dot{\epsilon}$, but the magnitude of the strain rate is commonly evaluated by the second invariant of \mathbf{D} without explicit calculation of the eigenvalues,

$$\mathbf{D} : \mathbf{D} = 2(1 - m + m^2)\dot{\epsilon}^2, \quad (4)$$

because it is always positive for finite values of $\dot{\epsilon}$ by definition. Since we are interested in the mode of the strain rate, or, equivalently, the value of m without solving the eigenvalue problem, we consider another invariant of \mathbf{D} . The determinant of \mathbf{D} , a third-order invariant, is expressed in terms of the eigenvalues by

$$\det \mathbf{D} = m(1 - m)\dot{\epsilon}^3. \quad (5)$$

From Eq. (5), we can see that the determinant of \mathbf{D} becomes zero for planar shear ($m = 1$), irrespective of $\dot{\epsilon}$. In other words, $\det \mathbf{D} = 0$ means that the strain directions are restricted to be within a certain plane, and $\det \mathbf{D} \neq 0$ indicates that the strain directions extend three-dimensionally. With this property of $\det \mathbf{D}$, we can get an insight into whether the local strain rate is more planar or more volumetric without explicitly calculating the eigenvalues of \mathbf{D} .

Combining Eqs. (4) and (5), we define a measure for the mode of the strain rate, independent of the value of $\dot{\epsilon}$, by

$$\beta = \frac{3\sqrt{6} \det \mathbf{D}}{(\mathbf{D} : \mathbf{D})^{3/2}}, \quad (6)$$

where the numerical prefactor is chosen so that the range of β is normalized to $[-1, 1]$. Special cases include: $\beta = -1$ for a biaxial elongational flow, $\beta = 1$ for a uniaxial elongational flow, and $\beta = 0$ for a planar shear flow. For the general case of $0 < |\beta| < 1$, the strain rate is an arbitrary superposition of an elongational flow and a shear flow. Both $\mathbf{D} : \mathbf{D}$ and $\det \mathbf{D}$ are frame invariant, implying that β is frame invariant as well, namely β does not change in different frames of the observers.

Now we consider a relation between the strain rate mode and the mixing capability. In general, if a mixing device has good mixing capability, the flow in the device should satisfy the following two conditions. (i) There exist some regions with large strain rates in order for the

materials to be stretched extensively. (ii) All the fluid elements in the mixer are efficiently and repeatedly conveyed to the large strain rate regions in order to have chances to be stretched. The distribution of the magnitude of the strain rate of Eq. (4) (or in the form of shear stress, $\eta(\mathbf{D} : \mathbf{D})\sqrt{\mathbf{D} : \mathbf{D}}$, with the shear viscosity η as a function of the magnitude of the strain rate) has often been discussed [8, 9, 17–22]. In mixing devices for highly viscous fluids, like polymers, the largest strain rate is achieved in narrow gap regions, which are the clearance between the screw/rotor tips and the barrel surface, and the gap between two screws/rotors in twin-shaft machines. Thus, it is usually the case the condition (i) is satisfied. However, it is only a necessary condition for good net mixing capability. These large strain rate regions are also responsible for the dispersion of agglomerates.

In contrast to the large strain rate regions, a role of regions with smaller strain rates on net distributive mixing is rather difficult to characterize because this would, in principle, require an analysis of the ensemble of trajectories. Nevertheless, the small strain rate regions are mainly responsible for the condition (ii). In the past, distributive mixing was discussed using tracer tracking and Lagrangian statistics [5, 7–9, 15, 16, 19, 23–28]. These methods are basically for the characterization of the global properties of a mixing device, and are not for the direct characterization of a relation between the local flow characteristics induced by a screw geometry and the mixing capability. Effective and repetitive transport of the materials to the large strain rate regions is one important role of the small strain rate region, and it affects net mixing performance of the mixers. This flow pattern structure in the small strain rate regions is basically based on the mixer geometry.

In order for the fluid elements to be stretched and folded over the whole space in a mixing device, the flow trajectories should be bifurcated and change directions with some frequency during the mixing process. This bifurcation of the flow trajectories is directly related to the volumetric modes of the strain rate. Therefore, the spatial distribution of the strain rate mode gives directly an insight into the relation between the mixing process and the flow driven by the mixer geometry.

For the characterization of the local deformation rate, there is another quantity, called the mixing index [29],

$$\lambda = \frac{\sqrt{\mathbf{D} : \mathbf{D}}}{\sqrt{\mathbf{D} : \mathbf{D}} + \sqrt{\boldsymbol{\Omega} : \boldsymbol{\Omega}^T}}, \quad (7)$$

which has often been used to characterize the efficiency of the dispersive mixing of mixing devices [17, 21, 22, 30, 31]. Some authors have used different normalization like $(\sqrt{\mathbf{D} : \mathbf{D}} - \sqrt{\boldsymbol{\Omega} : \boldsymbol{\Omega}^T}) / (\sqrt{\mathbf{D} : \mathbf{D}} + \sqrt{\boldsymbol{\Omega} : \boldsymbol{\Omega}^T})$ which takes a value in $[-1, 1]$ [13, 32] while λ is normalized to be within $[0, 1]$. Since $\boldsymbol{\Omega} : \boldsymbol{\Omega}^T$ is not frame invariant when the observer's frame depends on time, λ is not frame invariant in general. Nevertheless, if we choose a time inde-

pendent frame like the laboratory system of coordinates, λ is practically regarded as objective. By the definition in Eq. (7), λ defines the degree of irrotationality of the deformation rate, *e.g.*, $\lambda = 0$ for pure rotation, $\lambda = 1$ for an irrotational flow, and $0 < \lambda < 1$ for a partially rotational flow; furthermore, λ is independent of the strain rate mode. In two-dimensional flows, since available strain-rate mode is only planar elongational flow, irrotationality can be used to distinguish between simple shear flow ($\lambda = 1/2$) and elongational flow ($\lambda = 1$). However, this is not the case for three-dimensional flows since different strain-rate modes exist. In three-dimensional flows, λ simply indicates the irrotationality, but not the strain-rate mode. The mixing index λ and our measure for the strain rate mode β characterize different aspects of the local deformation rate.

III. NUMERICAL SIMULATION

The flow of a polymer melt in the melt-mixing zone of a twin-screw extruder has been numerically solved to allow understanding the relation between the distribution of the strain rate mode and the mixing capability of screw elements. The configuration of the screws is shown in Fig. 1. From the inlet, a forwarding conveying screw, kneading disks, and a backwarding conveying screw are arranged. The melt-mixing zone consists of kneading disks of neutrally staggered five blocks [33]. The diameter of the barrel is set to $D = 69$ mm, the length of the computational domain is $L = 2.92D$.

We focus on the situation where the material fully fills the channel. The Reynolds number is assumed to be much less than unity, so that inertial effects are neglected. The flow is assumed to be incompressible, and in a pseudo-steady state to screw rotation, as has often been assumed in polymer flow in twin-screw extruders [9, 11, 15, 19, 20, 22, 28, 34]. With these assumptions, the governing equations become

$$\nabla \cdot \mathbf{v} = 0, \quad (8)$$

$$0 = -\nabla p + \nabla \cdot \boldsymbol{\tau}, \quad (9)$$

$$\rho c_p \mathbf{v} \cdot \nabla T = k \nabla^2 T + \boldsymbol{\tau} : \mathbf{D}, \quad (10)$$

where p is the pressure, $\boldsymbol{\tau}$ is the deviatoric stress, ρ is the mass density, c_p is the specific heat capacity, T is the temperature, and k is the thermal conductivity.

The fluid is assumed to be a viscous shear-thinning fluid that follows Cross–Arrhenius viscosity [35],

$$\boldsymbol{\tau} = 2\eta\mathbf{D}, \quad (11)$$

$$\eta = \frac{\eta_0}{1 + c(\eta_0\dot{\gamma})^n}, \quad (12)$$

$$\eta_0 = a \exp\left(\frac{b}{T}\right), \quad (13)$$

$$\dot{\gamma} = \sqrt{2\mathbf{D} : \mathbf{D}}, \quad (14)$$

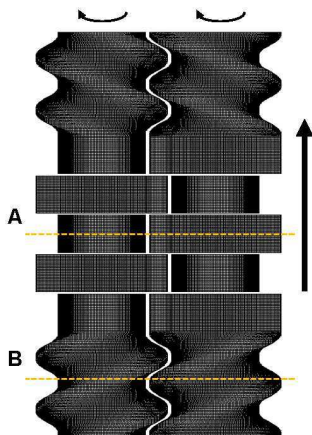


FIG. 1. Screw configuration of melt-mixing zone. From the inlet (bottom of the figure), forwarding conveying screw (FS), neutrally-staggered kneading disks (N-KD), and backwarding conveying screw (BS). The extrusion direction is indicated by the arrow on the right, while the rotation direction is indicated by the arrows on the top.

whose parameters are obtained by fitting the shear viscosity of a polypropylene melt taken from [34], and the values are $c = 1.3575 \times 10^{-3}$, $n = 0.66921$, $a = 1.7394$, and $b = 4656.8$. The mass density, specific heat capacity, and thermal conductivity are taken from [34] as well, and the values are $\rho = 735.0 \text{ kg/m}^3$, $c_p = 2100 \text{ J/(kg}\cdot\text{K)}$, and $k = 0.15 \text{ W/(m}\cdot\text{K)}$.

As operational conditions, the volume flow rate and the screw rotation speed are set to $60 \text{ cm}^3/\text{s}$ ($\approx 159 \text{ kg/h}$) and 200 rpm . The no-slip condition on the velocity at the barrel and screw surfaces is assumed. The velocity at the inlet boundary was set to a value under the given volume flow rate. The pressure at the outlet boundary was fixed to be a constant value. The temperatures on the barrel surface and at the inlet boundary were set to be a constant value of 473.15 K . The natural boundary conditions for the temperature equation in the exit boundary plane and the screw surface were assigned.

The set of equations was discretized by the finite volume method and solved by SIMPLE method [36] using a commercial software, “R-FLOW” (R-flow Co., Ltd., Saitama, Japan). From the obtained velocity field, the strain rate and the vorticity tensors were calculated so as to evaluate β and λ .

IV. RESULTS AND DISCUSSION

For typical twin-screw mixers, the largest strain rate occurs mainly around the tips and the gap between the two screws in the intermeshing region because the channel widths of these regions are designed to be the smallest in the device. This is common for the conveying screw of extruders and many types of kneading elements, such as

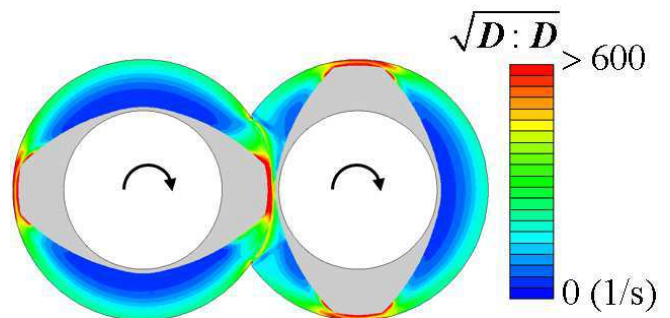


FIG. 2. Distribution of $\sqrt{\mathbf{D}:\mathbf{D}}$ as a typical magnitude of the strain rate at position B in Fig. 1. Large values of $\sqrt{\mathbf{D}:\mathbf{D}}$ over 600 (1/s) are reached at the narrow gaps between the screw tips and the barrel surface and between the two screws, while in the other regions, the value of $\sqrt{\mathbf{D}:\mathbf{D}}$ stays rather small.

kneading disks, rotor elements, screw mixing elements, and so on [5–11, 15, 17–20, 22, 28, 34, 37, 38]. To observe this, Fig. 2 shows the distribution of the magnitude of the strain rate, $\sqrt{\mathbf{D}:\mathbf{D}}$, at the cross section B indicated in Fig. 1. At the clearances between the screw-tips and the barrel surface, and the gap between two screws, $\sqrt{\mathbf{D}:\mathbf{D}}$ takes values larger than 600 (1/s) , which is consistent with the circumferential shear rate of 460 (1/s) estimated from the screw rotation speed of 200 rpm . In contrast, the magnitude of the strain rate in other regions is extremely small. The distribution of $\sqrt{\mathbf{D}:\mathbf{D}}$ is basically similar for the conveying screws and the kneading disks shown in Fig. 1, suggesting that the difference in the mixing capabilities of these elements are largely attributable to the differences in the flow patterns in the small strain rate regions.

Next, we compare the distributions of the volumetric strain rate between the conveying screw and the kneading disks. We use the absolute value of β as defining $d_v = |\beta|$, which is zero for a planar shear, unity for pure elongational flows, and becomes $0 < d_v < 1$ for an arbitrary superposition of planar and elongational flows, for we are interested in how the volumetric strain rate is distributed. Figure 3 shows the distributions of d_v at a cross section in the conveying screw (location B in Fig. 1) and at a cross section in the kneading disks (location A in Fig. 1). In the case of the conveying screw shown in Fig. 3(a), although an elongation flow occurs in some small regions around the tip-barrel clearance and in the intermeshing regions, small values of d_v prevail in most of the section. This was observed in the other phase of the screw rotation. From this observation, circumferential planar shear is predominant in the flow driven by a conveying screw, which corresponds to the flow along the screw root. The elongational flows around the tip-clearance regions in the conveying screw are explained as follows. When fluid elements go across a screw tip, that flow is a bifurcation from the upper stream flow along

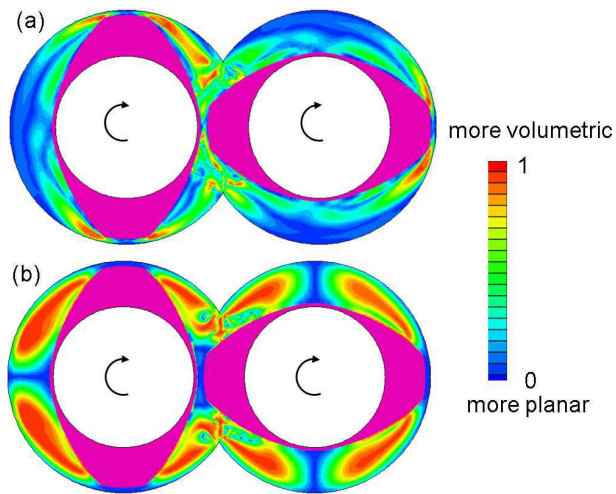


FIG. 3. Distributions of the degree of volumetric strain rate $d_v = |\beta|$ in the melt-mixing zone. The value of d_v is zero for a planar shear, unity for a pure elongational flow, and $0 < d_v < 1$ for a general flow. (a) The section in a conveying screw at position B in Fig. 1, (b) The section in the kneading disks at position A in Fig. 1.

the screw root, followed by the confluence to another flow along the next screw root. These flow patterns are observed as the elongational flows in Fig. 3(a). Except for these flow patterns, interchange of materials rarely occurs along screw rotations. This fact is consistent with the well-known low level of the mixing capability of a conveying screw, because a volumetric bifurcation of the trajectories rarely occurs, so that the distributive mixing is not much promoted.

In the case of the kneading disks shown in Fig. 3(b), we found that the volumetric strain rate develops in a remarkably large fraction of the section, and its distribution forms a characteristic pattern. Elongational flows occur in the region far from the screw tips and the surfaces, which are, coincidentally, small strain rate regions. The locations of the elongational flows correspond to those of the opening space between neighboring staggered disks. As demonstrated in Fig. 3, the distribution of the volumetric strain rate closely reflects the flow pattern structure caused by the geometric shapes of the elements, and characterizes the flow pattern in the small strain rate regions.

As for the kneading disks, the characteristic pattern in the distribution of d_v is supposed to be related to their known good mixing capability [5–7, 9, 11, 19]. For understanding the relation between the distribution of d_v and the mixing capability, we discuss the flow pattern in the small strain rate region in the kneading zone. Figure 4(a) shows the velocity field at the mid-plane of the channel at the third disk in the kneading zone. From Fig. 4(a), we see the flow trajectories from a tip to two neighboring disks along the screw rotation. Simultane-

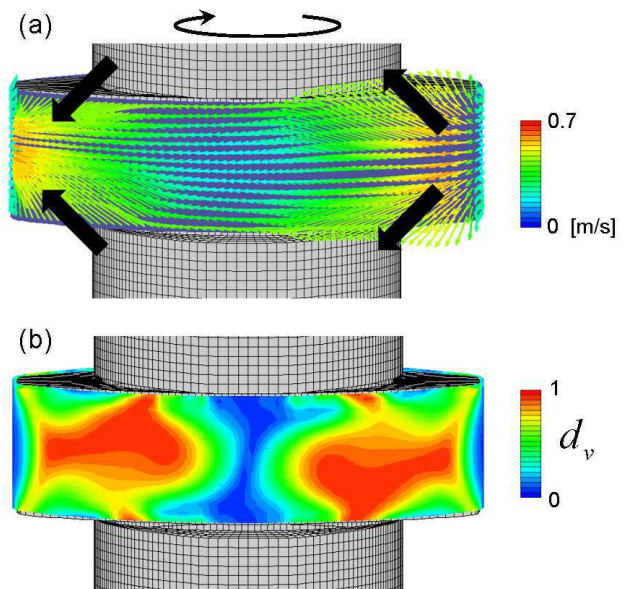


FIG. 4. Flow pattern in an internal section of a small strain rate region in the kneading disks: (a) velocity field, and (b) $d_v = |\beta|$ distribution. In (a), the thin arrows indicate the velocity field, while the big arrows are an eye-guide indicating the flow trends.

ously, converging flows from two neighboring disks are developed behind another side of screw tips. In other words, the flow driven by the kneading disks bifurcates into forward and backward extrusion directions on the one place and converges from neighboring disks on the other place. Because of these bifurcated trajectories, the fluid elements go back and forth within the zone of consecutively arranged disks, and repeatedly bifurcate and converge having many chances to be stretched and folded resulting in the high mixing capability of the kneading disks. This property of the flow pattern is reflected by the distribution of the biaxial/uniaxial elongational flow from the viewpoint of the strain rate mode. Figure 4(b) shows the distribution of d_v corresponding to the velocity field in Fig. 4(a) and clearly captures this characteristic flow pattern structure developed in the small strain rate region of the kneading disks. This analysis demonstrates that the volumetric strain rate distribution can be useful to characterize the flow pattern structure, especially in the small strain rate regions.

For comparison, the distribution of the mixing index (or the irrotationality), λ , of Eq. (7) at the cross sections A and B in Fig. 1 are shown in Fig. 5. We found that both the conveying screw and the kneading disks share some common characteristics in the λ distribution. The deformation rate is almost half rotational near the surfaces of the screws and the barrel, while it is almost irrotational in the small strain rate region far from the surfaces. Although the irrotational regions for both elements are different, depending on their geometric shapes,

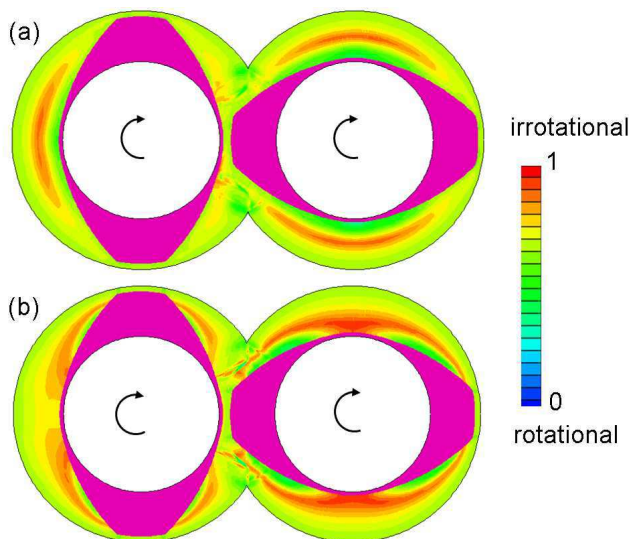


FIG. 5. Distributions of the irrotationality λ in the melt-mixing zone. The value of λ is zero for a pure rotation (or zero strain rate), and unity for an irrotational one. (a) The section in a conveying screw at position B in Fig. 1, (b) The section in the kneading disks at position A in Fig. 1.

the λ distribution does not reflect the flow pattern shown in Fig. 4(a), suggesting that the mixing index itself hardly offers insight into the flow pattern structure in general three-dimensional flow.

In order to discuss the large scale characteristics of the screw elements, d_v and λ are averaged in each section and over one screw rotation. The axial profiles of the mean d_v and λ are shown in Fig. 6. In proximity to the inlet and the outlet, the mean values are supposed to be affected by the boundary conditions, and so, physically irrelevant. We hence consider the axial locations from 20 mm to 200 mm. The means of d_v and λ remain at an almost constant level in the regions of the two conveying screws. In addition, these mean quantities do not vary much at the first and last blocks in the kneading disks because they are rather smoothly connected to the conveying screws. In contrast, the means of d_v and λ show large variation along the inner three blocks of the kneading disks. The piecewise variations of these values are due to the piecewise structure of the kneading disks. In particular, the variation in the mean d_v within the inner three blocks is remarkable. The mean d_v has a peak at the center of each of the three blocks, which reflects the bifurcated flow trajectories back and forth as observed in Fig. 4. The axial profile of the mean d_v clearly shows that the flow pattern structure specific to the kneading disks occurs in the inner blocks and originates from the consecutive staggered arrangement of the blocks. As demonstrated above, a flow pattern being effective for distributive mixing is closely related to the distribution of the volumetric strain rate which indicates three-dimensional bifurcation and converging of trajectory-

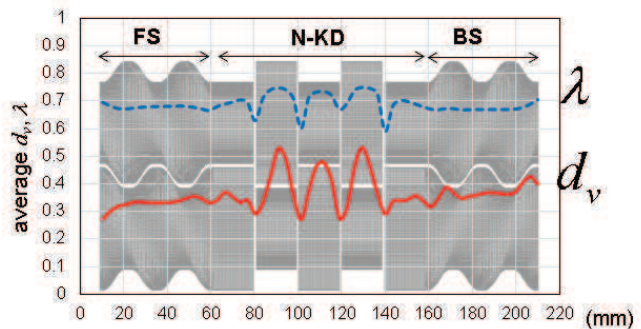


FIG. 6. Mean degree of volumetric strain rate and mean irrotationality (or mixing index) as functions of axial location. The values of d_v and λ are averaged spatio-temporally in sections perpendicular to the extrusion direction and over a period of one screw rotation. The region of each element, namely the forwarding conveying screw (FS), the neutrally-staggered kneading disks (N-KD), and the backwarding conveying screw (BS), are indicated by the left right arrow.

ries. The distribution of d_v offers a physical insight into the high mixing capability of the kneading disks as well as the low mixing capability of the conveying screws.

V. CONCLUSIONS

We derived a scalar measure, β , which characterizes the mode of the local strain rate by combining the second and the third invariants of the strain rate tensor. Using the value of β , the mode of the strain rate tensor including a uniaxial/biaxial elongational flow, a planar shear flow, and arbitrary combinations, is defined for the general three-dimensional flows observed in fluid mechanical processes without solving the eigenvalue problem for the strain rate tensor.

The spatial distribution of non-planar, or volumetric, strain rate is closely related to the flow patterns, irrespective of the magnitude of the strain rate, and therefore it was found to be useful to understand the relation between the mixer geometry and the flow pattern structures. From the viewpoint of mixing processes, the flow pattern in the small strain rate regions has an important role in efficient and repetitive transport of the fluid elements to the large strain rate regions in order to enhance the net mixing capability of the mixer. For understanding the effectiveness of the flow pattern especially in the small strain rate regions, the distribution of the volumetric strain rates can be a useful tool. Based on the numerical simulation of a melt-mixing flow in twin-screw extrusion, flows driven by the conveying screws and the kneading disks have been analyzed. We found that the flow patterns specific to these elements are clearly characterized by the distribution of the strain rate mode.

Understanding the relation between the geometric structure of the mixing elements and the flow pattern they drive is an important issue in the essential evaluation of the mixing capability of the mixing devices used in different industries. The analysis employing the strain rate mode and its distribution is effective for discussing the flow pattern in the mixing device and offers an insight into the role of the small strain rate regions on the distributive mixing.

Finally, we would like to mention a limitation of the analysis only by β for the mixing. Although the distribution of the volumetric strain rates can give information about the flow pattern structures specifying the regions where the flow bifurcates and converges, it can just distinguish the potential of particular flows. For direct evaluation of the mixing, kinetic evolution of interface is needed to discuss the area growth, interface folding, and material distribution. Computation of the interface kinetics requires the directions of the area segments, and therefore the mixing is a function of the orientation of

the interface relative to the flow. This aspect of the mixing is another important problem from the evaluation of the potential of the flow. The combined use of our measure for the strain rate mode with other fluid mechanical analyses, including kinetic evolution of area elements is an important future direction of research into predicting the mixing capabilities of different mixing elements and in designing improved novel mixing elements.

ACKNOWLEDGMENTS

The numerical calculations have been partly carried out using the computer facilities at the Research Institute for Information Technology at Kyushu University. This work has been supported by Grants-in-Aid for Scientific Research (JSPS KAKENHI) under Grants Nos. 26400433, 24656473, and 15H04175.

-
- [1] Tadmor Z, Gogos CG. *Principles of Polymer Processing*. New Jersey: Wiley-Interscience, 2nd ed. 2006.
- [2] White JL, Kim EK. *Twin Screw Extrusion Technology and Principles*. Munich: Hanser. 2010.
- [3] Aguilera JM, Barbosa-Canovas GV, Simpson R, Welti-Chanes J, Bermudez-Aguirre D, eds. *Food Engineering Interfaces*. New York: Springer. 2011.
- [4] Rauwendaal C. *Polymer Extrusion*. Munich: Hanser, 5th ed. 2014.
- [5] Lawal A, Kalyon DM. Mechanisms of mixing in single and co-rotating twin screw extruders. *Polym Eng Sci*. 1995;35(17):1325–1338.
- [6] Carneiro OS, Caldeira G, Covas JA. Flow patterns in twin-screw extruders. *J Mater Process Tech*. 1999;92-93:309–315.
- [7] Funatsu K, Kihara SI, Miyazaki M, Katsuki S, Kajiwara T. 3-D numerical analysis on the mixing performance for assemblies with filled zone of right-handed and left-handed double-flighted screws and kneading blocks in twin-screw extruders. *Polym Eng Sci*. 2002;42(4):707–723.
- [8] Ishikawa T, Amano T, Kihara SI, Funatsu K. Flow patterns and mixing mechanisms in the screw mixing element of a co-rotating twin-screw extruder. *Polym Eng Sci*. 2002;42(5):925–939.
- [9] Zhang XM, Feng LF, Chen WX, Hu GH. Numerical simulation and experimental validation of mixing performance of kneading discs in a twin screw extruder. *Polym Eng Sci*. 2009;49(9):1772–1783.
- [10] Kubik P, Vlcek J, Tzoganakis C, Miller L. Method of analyzing and quantifying the performance of mixing sections. *Polym Eng Sci*. 2012;52(6):1232–1240.
- [11] Sarhangi Fard A, Anderson PD. Simulation of distributive mixing inside mixing elements of co-rotating twin-screw extruders. *Comput Fluids*. 2013;87:79–91.
- [12] Ottino JM, Ranz WE, Macosko CW. A lamellar model for analysis of liquid-liquid mixing. *Chem Eng Sci*. 1979; 34(6):877–890.
- [13] Ottino JM. *The Kinematics of Mixing*. Cambridge, UK: Cambridge University Press. 1989.
- [14] Manas-Zloczower I, Cheng H. Analysis of mixing efficiency in polymer processing equipment. *Macromol Symp*. 1996;112(1):77–84.
- [15] Nakayama Y, Takeda E, Shigeishi T, Tomiyama H, Kajiwara T. Melt-mixing by novel pitched-tip kneading disks in a co-rotating twin-screw extruder. *Chem Eng Sci*. 2011;66(1):103–110.
- [16] Connelly RK, Kokini JL. Examination of the mixing ability of single and twin screw mixers using 2D finite element method simulation with particle tracking. *J Food Eng*. 2007;79(3):956–969.
- [17] Yao CH, Manas-Zloczower I. Influence of design on dispersive mixing performance in an axial discharge continuous mixer - LCMAX 40. *Polym Eng Sci*. 1998;38(6):936–946.
- [18] Alsteens B, Legat V, Avalosse T. Parametric Study of the Mixing Efficiency in a Kneading Block Section of a Twin-screw Extruder. *Intern Polym Process*. 2004;19:207–217.
- [19] Bravo VL, Hrymak AN, Wright JD. Study of particle trajectories, residence times and flow behavior in kneading discs of intermeshing co-rotating twin-screw extruders. *Polym Eng Sci*. 2004;44(4):779–793.
- [20] Malik M, Kalyon DM. 3D Finite Element Simulation of Processing of Generalized Newtonian Fluids in Counter-rotating and Tangential TSE and Die Combination. *Intern Polym Process*. 2005;20(4):398–409.
- [21] Connelly RK, Kokini JL. 3D numerical simulation of the flow of viscous newtonian and shear thinning fluids in a twin sigma blade mixer. *Adv Polym Technol*. 2006; 25(3):182–194.
- [22] Rathod ML, Kokini JL. Effect of mixer geometry and operating conditions on mixing efficiency of a non-Newtonian fluid in a twin screw mixer. *J Food Eng*. 2013; 118(3):256–265.
- [23] Lawal A, Kalyon DM. Simulation of intensity of segregation distributions using three-dimensional fem analysis:

- Application to corotating twin screw extrusion processing. *J Appl Polym Sci.* 1995;58(9):1501–1507.
- [24] Yao WG, Takahashi K, Abe Y. Analytical Study on Flow and Distributive Mixing of a New Type Pin Mixing Section for Screw Extruder. *Intern Polym Process.* 1996; 11(3):222–227.
- [25] Yao WG, Takahashi K, Koyama K, Dai GC. Design of a new type of pin mixing section for a screw extruder based on analysis of flow and distributive mixing performance. *Chem Eng Sci.* 1997;52(1):13–21.
- [26] Cheng H, Manas-Zloczower I. Distributive mixing in conveying elements of a ZSK-53 co-rotating twin screw extruder. *Polym Eng Sci.* 1998;38(6):926–935.
- [27] Yao WG, Tanifuji S, Takahashi K, Koyama K. Mixing efficiency in a pin mixing section for single-screw extruders. *Polym Eng Sci.* 2001;41(6):908–917.
- [28] Hirata K, Ishida H, Hiragohri M, Nakayama Y, Kajiwara T. Effectiveness of a backward mixing screw element for glass fiber dispersion in a twin-screw extruder. *Polym Eng Sci.* 2014;54(9):2005–2012.
- [29] Cheng JJ, Manas-Zloczower I. Flow Field Characterization in a Banbury Mixer. *Intern Polym Process.* 1990; 5(3):178–183.
- [30] Yang HH, Manas-Zloczower I. Flow field analysis of the kneading disc region in a co-rotating twin screw extruder. *Polym Eng Sci.* 1992;32(19):1411–1417.
- [31] Cheng H, Manas-Zloczower I. Study of mixing efficiency in kneading discs of co-rotating twin-screw extruders. *Polym Eng Sci.* 1997;37(6):1082–1090.
- [32] Jongen T. Characterization of batch mixers using numerical flow simulations. *AIChE J.* 2000;46(11):2140–2150.
- [33] Kohlgruber K. *Co-Rotating Twin Screw Extruder.* Munich: Hanser. 2008.
- [34] Ishikawa T, Kihara SI, Funatsu K. 3-D numerical simulations of nonisothermal flow in co-rotating twin screw extruders. *Polym Eng Sci.* 2000;40(2):357–364.
- [35] Cross MM. Rheology of non-Newtonian fluids: A new flow equation for pseudoplastic systems. *J Colloid Sci.* 1965;20(5):417–437.
- [36] Versteeg H, Malalasekera W. *An Introduction to Computational Fluid Dynamics: The Finite Volume Method (2nd Edition).* Harlow, England: Prentice Hall, 2nd ed. 2007.
- [37] Kalyon DM, Malik M. An Integrated Approach for Numerical Analysis of Coupled Flow and Heat Transfer in Co-rotating Twin Screw Extruders. *Intern Polym Process.* 2007;22(3):293–302.
- [38] Vyakaranam KV, Kokini JL. Prediction of air bubble dispersion in a viscous fluid in a twin-screw continuous mixer using FEM simulations of dispersive mixing. *Chem Eng Sci.* 2012;84:303–314.